Received: 25 September 2017 | Revised: 9 April 2018 | Accepted: 9 April 2018

DOI: 10.1002/hbm.24197

WILEY

RESEARCH ARTICLE

Functional connections between activated and deactivated brain regions mediate emotional interference during externally directed cognition

Simone Di Plinio[1] | Francesca Ferri[2] | Laura Marzetti[1,3] | Gian Luca Romani[1,3] | Georg Northoff[4,5] | Vittorio Pizzella[1,3]

[1]Department of Neuroscience Imaging and Clinical Sciences, "G. D'Annunzio" University of Chieti-Pescara, Chieti 66100, Italy

[2]Centre for Brain Science, Department of Psychology, University of Essex, Colchester CO4 3SQ, United Kingdom

[3]Institute for Advanced Biomedical Technologies, Chieti 66100, Italy

[4]Institute of Mental Health Research, University of Ottawa, Ottawa, Ontario K1Z 7K4, Canada

[5]Zhejiang University School of Medicine, Mental Health Centre, Hangzhou, China

Correspondence
Simone Di Plinio, Department of Neuroscience Imaging and Clinical Sciences, "G. D'Annunzio" University of Chieti-Pescara, Chieti 66100, Italy.
Email: simonediplinio@yahoo.it

Abstract

Recent evidence shows that task-deactivations are functionally relevant for cognitive performance. Indeed, higher cognitive engagement has been associated with higher suppression of activity in task-deactivated brain regions - usually ascribed to the Default Mode Network (DMN). Moreover, a negative correlation between these regions and areas actively engaged by the task is associated with better performance. DMN regions show positive modulation during autobiographical, social, and emotional tasks. However, it is not clear how processing of emotional stimuli affects the interplay between the DMN and executive brain regions. We studied this interplay in an fMRI experiment using emotional negative stimuli as distractors. Activity modulations induced by the emotional interference of negative stimuli were found in frontal, parietal, and visual areas, and were associated with modulations of functional connectivity between these task-activated areas and DMN regions. A worse performance was predicted both by lower activity in the superior parietal cortex and higher connectivity between visual areas and frontal DMN regions. Connectivity between right inferior frontal gyrus and several DMN regions in the left hemisphere was related to the behavioral performance. This relation was weaker in the negative than in the neutral condition, likely suggesting less functional inhibitions of DMN regions during emotional processing. These results show that both executive and DMN regions are crucial for the emotional interference process and suggest that DMN connections are related to the interplay between externally-directed and internally-focused processes. Among DMN regions, superior frontal gyrus may be a key node in regulating the interference triggered by emotional stimuli.

KEYWORDS

attention, cognitive interference, default mode network, deactivations, emotions, functional magnetic resonance imaging, functional connectivity, neuroimaging, working memory

1 | INTRODUCTION

Under cognitive demand, two neurophysiological events occur in the brain: on one hand, specific brain areas related to task execution show activations (Cabeza, 2000; Raichle, 1998); on the other hand, different brain regions show negative drifts in the BOLD activity with respect to the baseline (i.e., deactivations, Shulman et al., 1997, Fox et al., 2005). Brain regions that consistently show a deactivation during externally-directed attention are often referred to as "task-negative" regions (Fox et al., 2005). The same areas are highly connected during the resting state (Greicius, Krasnow, Reiss, & Menon, 2003), a condition in which the subject is not engaged in any specific task and the brain is expected to be in an uncontrolled state with a highly variable flow of thoughts (Supek & Aine, 2014). Despite the expected variability, the topography of these highly interconnected regions is similar across subjects and comprises the so-called default mode network (DMN, Gusnard & Raichle, 2001). Regions of the DMN can exhibit increased activity both in internally focused processes (e.g., autobiographic tasks) and during emotional stimulation (Bado et al., 2014; Buckner, Andrews-Hanna, & Schacter, 2008; Fox, Spreng, Ellamil, Andrews-Hanna, & Christoff,

2015). Thus, it is more reasonable to refer to brain regions as "task-activated" or "task-deactivated" more than "task-positive" or "task-negative" (Spreng, 2012). In fact, task-related activations and deactivations are likely to be task-specific phenomena (Leech et al., 2014), and the externally directed or self-focused nature of the task may lead to different spatial extents of the two processes (Andrews-Hanna, Smallwood, & Spreng, 2014).

The interplay between activations and deactivations plays a crucial role in cognition (Elton & Gao, 2015; Northoff et al., 2004), but the factors affecting such interplay are still unclear. Indeed, while it has been demonstrated that the task engagement is reflected in task-related deactivations (Singh & Fawcett, 2008) and that stronger anticorrelations (Buckner, Krienen, & Yeo, 2013) between the DMN and executive regions favor higher performance (Hampson, Driesen, Roth, Gore, & Constable, 2010; Kelly, Uddin, Biswal, Castellanos, & Milham, 2008), it is still unclear how the interplay between activations and deactivations is remodeled when emotional stimuli are perceived. The neural correlates of emotions have been studied in the past with an emphasis on limbic and executive prefrontal regions, often observing opposing effects on executive control regions (Cohen & Henik, 2012; Dolcos, Wang, & Mather, 2014). However, the involvement of the DMN in self-focused tasks (Li, Wang, Yao, Hu, & Friston, 2012) and emotional manipulations (McRae et al., 2010; Ochsner, Silvers, & Buhle, 2012) suggests that this network is an ideal candidate for understanding how externally directed attention is affected when the perceived stimuli have emotional features. Moreover, while there are well-known connections between emotional stimuli and the limbic system, as well as between DMN regions and the limbic system (Catani, Dell'acqua, & Thiebaut de Schotten, 2013), the link between emotions and the DMN remains unclear.

To understand how emotional visual stimuli lead to modulations in activity and functional connectivity between task-activated and task-deactivated regions during externally-directed attention, we used an fMRI delayed match-to-sample task in which subjects do not have to pay attention to the emotional content but only to the shape of the visual stimulus. Thus, we produce an emotional interference effect inferred by irrelevant emotional features of the visual stimulus. This emotional interference is likely to be reflected both by the worsening of the behavioral performance and by modulations in brain activity and connectivity.

Our hypotheses are that (a) the emotional interference causes activity modulations in brain regions actively engaged by the execution of externally focused tasks and (b) these modulations are associated with changes in the functional connections between these areas and deactivated (DMN) regions related to internally focused processes. These changes in functional connectivity would explain the higher cognitive interference and the worse behavioral performance caused by emotional stimuli. Previous studies of emotional interference demonstrated that subjects could ignore emotional distractors and pay attention to specific features of the stimulus (Most, Chun, Johnson, & Kiehl, 2006, Codispoti et al., 2015). In this way, resources are drawn away from the ongoing task, and the performance is disrupted (Buodo, Sarlo, & Palomba, 2002; Schimmack, 2005; Kennedy et al., 2015). In our case, the choice of an orthogonal paradigm is also useful to avoid confounds due to different strategies of emotional reappraisal (Gutentag, Halperin, Porat, Bigman, & Tamir, 2016) and to reduce the habituation effect (Carretié, Hinojosa, & Mercado, 2003) while solving an externally focused task. Neutral and negative stimuli were defined through a dimensional approach to the study of emotions (Hamann, 2012; Russell, 2009), and experimental conditions were individualized to account for interindividual differences in the subjective perception of emotional stimuli (Lindquist & Barrett, 2012). To obtain a mask of task-related regions, that is, regions involved in the match-to-sample task regardless of the emotional content of the stimuli, we used a third condition with visual noise as stimuli. We investigated three effects of the emotional interference. First: do task-related brain regions show an activity modulation related to the emotional interference during externally directed attention? Second is the emotional interference reflected in specific shifts of functional connectivity between task-activated and task-deactivated regions? Third is how these modulations are related to the worsening of the behavioral performance?

2 | MATERIALS AND METHODS

2.1 | Task procedure

Twenty healthy Italian subjects (mean age 21 ± 1 years; 10 males, 10 females) participated in the fMRI study. None of the participants had ever suffered from any psychiatric or neurological disease, and none had any contraindication for MRI scanning. Among participants, 18 were right-handed, and 2 were left-handed. All subjects gave written informed consent before taking part in the study. The experiment was approved by the local ethics committee.

Visual stimuli used in the experiment were polygons with an odd number of edges that could vary from 9 to 19. Inside the polygon, an image was embedded. The image could represent either visual noise or a real image extracted from the "People" subset of the Nencki Affective Picture System (NAPS) database (Marchewka, Żurawski, Jednoróg, & Grabowska, 2014). These images represented visibly alive, injured, or dead human bodies or isolated parts of the human body. Images of the NAPS database are balanced for luminance and for other physical proprieties. The visual noise was obtained by randomly scrambling the pixels of these images.

Participants performed a delayed match-to-sample task (Figure 1): in each trial, they had to indicate if a second stimulus (target) had the same shape of the first stimulus (sample). Sample and target presentation lasted 1.71 s. Participants were instructed to press a button with their left index, if the shape was identical, or to press a button with their right index, if the shape changed. The delay between sample and target was jittered between 3.42 and 5.13 s. During the delay period, participants were instructed to fix a cross located in the center of the screen. After the target, a blank screen lasting between 8 and 12 s (inter trial interval, ITI) was presented. In one-half of the trials, the number of edges in the polygon of the target was different from that of the sample stimulus (*change* trials), while in the other half the same number of edges characterized the polygons in the sample and target stimuli

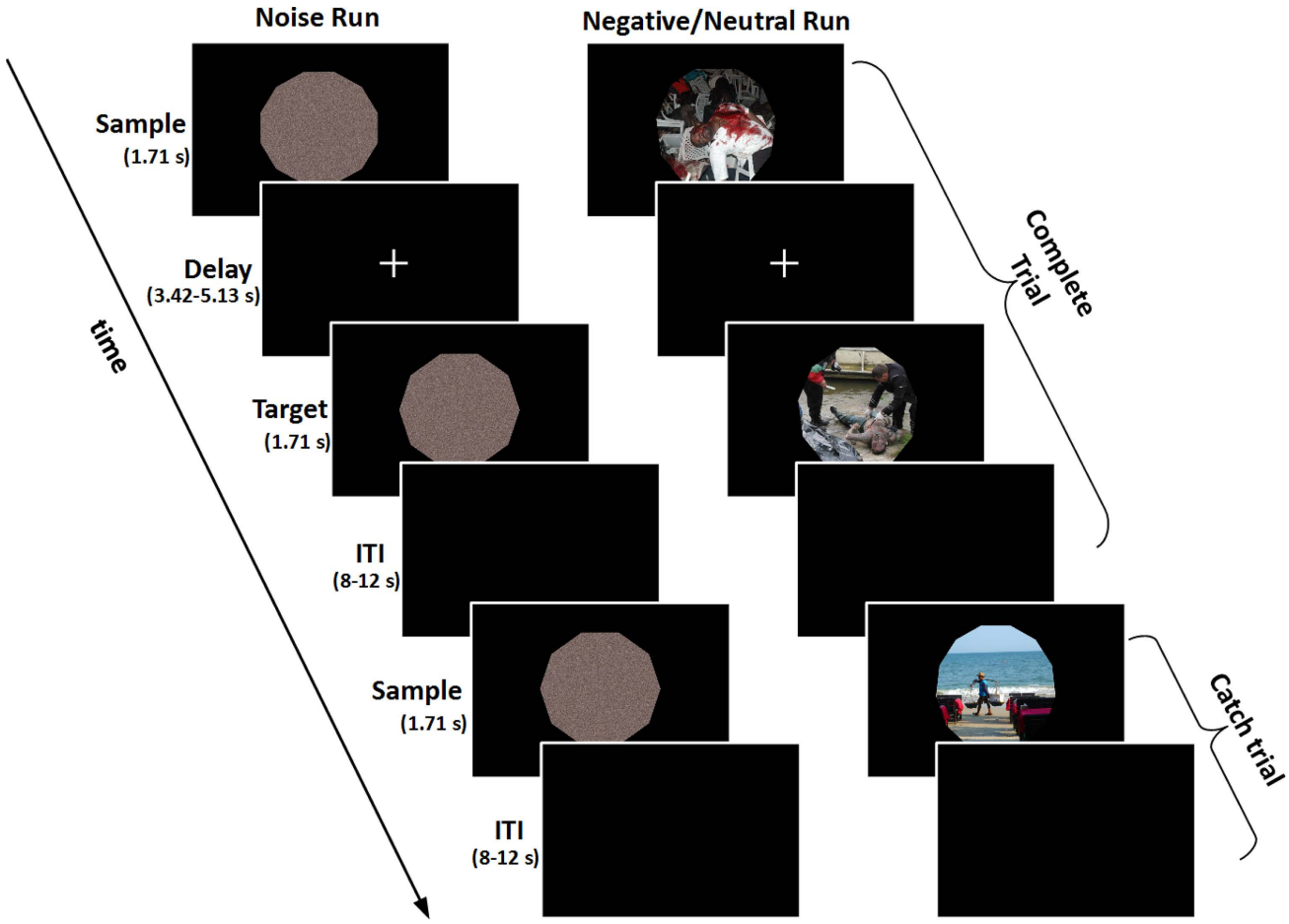

FIGURE 1 Task procedure. An example of each type of trial, for each run, is illustrated. Both during noise and negative/neutral runs, complete trials consisted of four periods: the sample presentation, a jittered delay period, the target presentation (during which subjects performed the behavioral response), and a jittered Inter Trial Interval (ITI). Catch trials consisted of the presentation of a sample stimulus directly followed by ITI, thus, requiring no behavioral response [Color figure can be viewed at wileyonlinelibrary.com]

(*same* trials). Catch trials were introduced to identify regions modulated by the emotional content of the sample stimulus alone. Indeed, in catch trials, sample stimuli were followed by a blank screen. Therefore, no behavioral response was required.

2.2 | Preliminary group rating

To consider possible socio-cultural differences in emotional perception (Grossmann, Ellsworth, & Hong, 2012), a preliminary group rating was conducted using the overall subset (250 images) on an independent group of 20 Italian participants (mean age 21 ± 2 years; 10 males, 10 females). During this procedure, ratings of valence, arousal, and avoidance-approach were collected for each image, as described in Marchewka et al. (2014). Given the possible differences between males and females perception of emotional stimuli (Biele & Grabowska, 2006; Filkowski, Olsen, Duda, Wanger, & Sabatinelli, 2017), images for which the score of valence or arousal differed significantly between males and females were excluded ($N = 48$). This difference was estimated using two-samples t tests (threshold: $p < .05$). To avoid the presentation of ambiguous stimuli, images showing a high standard deviation (>2) in the rating of valence or arousal were also excluded ($N = 8$).

This preliminary rating led to the selection of 40 negative images (mean valence: 2.31 ± 0.36; mean arousal: 7.11 ± 0.42; mean avoidance-approach: 3.90 ± 0.76) and 40 neutral images (mean valence: 5.50 ± 0.58; mean arousal: 4.46 ± 0.51; mean avoidance-approach: 5.43 ± 0.54), which were used as stimuli in the *negative* and *neutral* conditions, respectively. Images were presented in pseudorandomized order. Each neutral and negative picture was presented three or four times during the task, with the following restrictions: at least five other images of the same condition were interposed between the presentations of the same image; the same condition could not be presented more than three times consequently.

2.3 | fMRI session

During the scan sessions, participants performed four runs of the delayed match-to-sample task. In two of the four runs, the stimuli embedded into the polygons consisted of visual noise, obtained by shuffling the pixels of the NAPS images; a total of 48 complete noise trials and 48 noise catch trials were performed by each subject. In the other two runs, stimuli embedded into the polygons could have been either negative or neutral images; a total of 48 complete trials and

24 catch trials for each of the two conditions (negative, neutral) were performed by each subject in these neutral/negative runs. Noise and neutral/negative runs lasted about 12 and 19 min, respectively, and their order was counterbalanced across participants. After the fMRI session, each subject rated the neutral and negative images, thus allowing the collection of individual ratings of valence, arousal, and avoidance-approach.

2.4 | Individual rating and task complexity

We used the individual ratings collected after the fMRI session to score the NAPS images and label negative and neutral trials and to consider interindividual variability in emotion perception. A Principal Component Analysis (PCA) was used to identify principal components from the emotional dimensions of valence and arousal, across all the 80 images and across participants (for the usage of PCA methods to reduce data dimensionality, see Gorban, Kégl, Wunsch, & Zinovyev, 2008). The first component accounted for 92% of the variance and was used to distinguish between individual neutral and negative images. We refer to this component as the *valence*arousal* dimension. For each subject, we considered as neutral only images with a score above the subject's mean score in *valence*arousal*. Images with a score equal or below the subject's mean score were considered as negative. Accordingly, for each subject, we considered as neutral only trials in which both sample and target stimuli were neutral images, while only trials in which both sample and target stimuli were negative images were considered as negative. Trials in which one image was negative and the other one was neutral were labeled as "mix" trials but were not investigated due to their low number.

Stimulus complexity, represented by the number of edges of the polygon in which the images were embedded, was individualized after a preliminary behavioral session (1–3 days before the fMRI scan). In this session, each subject performed the delayed match-to-sample task at various difficulty levels, but only with noisy images. For each subject, the final difficulty level was set to achieve a performance close to 0.75, thus allowing a similar cognitive load at each subject during the scan session. Subjects with a mean score below the chance level (<0.50) at all difficulty levels were excluded from the experiment. This procedure was applied to avoid an effect of the task-difficulty on the strength of task-induced deactivations (Singh & Fawcett, 2008).

2.5 | Data acquisition

Functional MRI scans were acquired using the 3T Siemens Achieva scanner installed at the Institute for Advanced Biomedical Technologies (Gabriele D'Annunzio University, Chieti-Pescara, Italy), equipped with a standard receiver head coil. Whole brain functional images were acquired with a gradient echo-planar sequence using the following parameters: repetition time (TR) = 1,710 ms, echo time (TE) = 30 ms, field of view (FoV) = 230 mm^2, flip angle = 65°, voxel size = 3.6 mm^2, slice thickness = 5 mm. Each noise run included 414 volumes, while each negative/neutral run included 663 volumes. A high-resolution T1-weighted whole brain image was also acquired after functional sessions, via a 3D-MPRAGE sequence with the following parameters: TR = 8.1 ms, TE = 3.7 ms, FoV = 240 mm^2 flip angle = 8°, in-plane voxel size = 1 mm^3, slice thickness = 1 mm^3. The stimulus delivery was controlled by the E-Prime software (Schneider, Eschman, & Zuccolotto, 2012). Behavioral responses were recorded using a Cedrus Lumina pad system interfaced with the stimulus presentation PC.

2.6 | Behavioral differences between negative and neutral trials

A repeated measures 2 × 2 ANOVA with factors *emotion* (levels: negative, neutral) and *trial type* (levels: same, change) was used to estimate differences in accuracy and Reaction Times (RT) between conditions. ANOVAs were run both using trial classification according to group ratings and individual ratings. We compared the effect sizes of standard and individualized subdivisions in estimating differences between neutral and negative conditions using the omega squared measure of effect size (ω^2), which is considered a less biased effect size estimator than eta squared (η^2, Olejnik & Algina, 2003; Troncoso Skidmore & Thompson, 2013):

$$\omega^2 = (SS_{emo} - df_{emo} * MSE)/(SS_{tot} + MSE),$$

where SS is the sum of squares, df_{emo} are the degrees of freedom for the emotion factor ($df_{emo} = 1$), and MSE is the mean squared error.

We performed a control analysis, dividing negative/neutral conditions into four temporal blocks. Each block consisted of a quarter of the overall trials. For both negative and neutral conditions, the mean performance (accuracy and RT) was calculated in each block for each participant. We then ran a 2 × 4 ANOVA using *emotion* (levels: neutral, negative) and *block* (levels: B1, B2, B3, B4) as factors. This analysis aimed at evaluating if the effect of the emotional interference was different between early and late trials.

Behavioral differences in reaction time (ΔRT) that represent the behavioral effect of the emotional interference were calculated for each subject as the difference between the mean RT in negative trials and the mean RT in neutral trials: $\Delta RT = RT_{neg} - RT_{neu}$.

2.7 | fMRI data analysis

2.7.1 | Preprocessing

Preprocessing steps of functional data were implemented in AFNI (Cox, 1996). A slice-timing correction was applied to remove differences in acquisition times between slices. Functional images were deobliqued, despiked, and motion corrected using a six-parameter rigid body realignment. Anatomical and functional images were co-registered and stereotactically normalized to Talairach space (Talairach & Tournoux, 1988). A Gaussian filter of 6 mm full-width at half-maximum was applied to spatially smooth the functional images. Three subjects were excluded because of excessive head motion or poor response rates during scanning, leaving a final sample size of 17 (15 right-handed and 2 left-handed).

2.7.2 | Definition of a task-related mask

As our aim was to evaluate the modulations caused by emotional interference in regions significantly activated/deactivated by task execution,

we extracted the pattern of such modulations in a nonemotional context of the same task, that is, during noise runs. The hemodynamic function response was estimated using a finite impulse response (FIR) model, via the TENTzero basis function implemented in AFNI. The hemodynamic shape was modeled from 1.6 to 12.8 s after the sample onset using a set of 8 basis functions that represented the eight timepoints that covered the whole trial. Correct trials, catch trials, and incorrect trials were modeled separately, leading to a total of three regressors in the general linear model (GLM): sample onset in correct trials, sample onset in incorrect trials, sample onset in catch trials. Motion parameters obtained during preprocessing, as well as the signal extracted from white matter and cerebrospinal fluid, were used as additional nuisance regressors.

A one-sample *t* test on the mean estimated activity in correct noise trials, excluding the first and the last timepoints, was used to identify voxels significantly modulated by the task, namely task-related voxels. Task-activated voxels were defined as the task-related voxels in which the mean activity was significantly higher than the baseline, while task-deactivated voxels were defined as the task-related voxels in which the mean activity was significantly lower than the baseline. Notably, the baseline included (a) the mean level of the signal; (b) slow drifts; (c) motion parameters; and (d) cerebrospinal fluid and white matter signals.

Results were corrected via Monte Carlo simulation as implemented in the AFNI program 3dClustSim, using a threshold of $p < .005$ and a cluster size >100 voxels, to obtain a corrected significance level of $\alpha < 0.05$. To note, the power of cluster size corrections using the updated version of 3dClustSim, especially high for event-related studies, has been confirmed in a recent paper by (Cox, Chen, Glen, Reynolds, & Taylor, 2017). The activations and deactivations obtained through noise trials were used as a task-related mask for the following analyses of task-induced activity and functional connectivity.

2.7.3 | Activity in neutral and negative trials

Only voxels located in the task-related mask, as defined using noise trials were included in the following analysis. Negative and neutral conditions were separately modelled and one regressor was included for mix trials, leading to a total of 7 regressors in the GLM: sample onset in correct trials (neutral and negative), sample onset in incorrect trials (neutral and negative), sample onset in catch trials (neutral and negative), sample onset in mix trials. As for noise trials, activity in negative and neutral trials was estimated using the TENTzero model. Motion parameters, white matter signal, and cerebrospinal fluid signal were used as additional nuisance regressors. Only correct trials were considered.

To compare activations in neutral and negative conditions at the group level, we used a multivariate model (Chen, Saad, Adleman, Leibenluft, & Cox, 2015) including *emotion* (levels: negative, neutral) and *timepoint* (levels: T1, T2, T3, T4, T5, T6, T7, T8) as factors. The independent variable in the model was the β value which represented the estimated activation in each condition and each timepoint. We ran this model separately for complete trials and catch trials, to detect subtle modifications of the estimated hemodynamic function shape in response to both the task execution and the stimulus presentation alone. Results were corrected via Monte Carlo simulation as implemented in the AFNI program 3dClustSim, using a threshold of $p < .005$ and a cluster size >50 voxel, to obtain a corrected significance level of $\alpha < 0.05$.

To visualize activity in the modulated regions, we constructed a Region of Interest (RoI) around the center of mass of each cluster. Each RoI consisted of a 6-mm-radius sphere. Subsequently, we extracted the activity as the mean value across voxels included in each RoI, separately for correct negative and neutral trials. For each RoI and timepoint, we compared activations in neutral and negative conditions using paired t-tests. For each modulated timepoint, we estimated the difference in activity between conditions by subtracting the neutral β value from the negative one: $\Delta\beta_{act} = \beta_{neg} - \beta_{neu}$. To understand how brain activity modulations are related to inter-individual variability in emotional interference, for significantly modulated timepoints we estimated correlations between behavioral differences (ΔRT) and differences in the estimated activity ($\Delta\beta_{act}$). Results have been corrected for multiple comparisons using false discovery rate (FDR, Benjamini & Hochberg, 1995).

2.7.4 | Functional connectivity analysis

Functional connectivity between modulated task-activated ROIs and task-deactivated voxels was calculated for neutral and negative conditions using the generalized procedure of psycho-physiological interactions (gPPI, see McLaren, Ries, Xu, & Johnson, 2012). To account for all sources of variability, the new regression model also included gPPI regressors, the seed's extracted activity, and all the original 7 regressors used in the timeline analysis. Therefore, the model comprised a total of 15 regressors of interest, as well as nuisance regressors for motion, white matter, and cerebrospinal fluid.

As seeds for the gPPI analyses, we used the 6-mm-radius spheres centered in the center of mass of the clusters which showed a significant modulation between neutral and negative conditions. A GLM was run independently for each seed. In line with our purposes, functional connectivity was estimated between each seed and the task-related mask extracted using noise runs.

Effect of emotion

To detect differences in functional connectivity between neutral and negative conditions, connectivity maps from gPPI were analyzed using a linear mixed-effects model (Chen, Saad, Britton, Pine, & Cox, 2013) in which *emotion* was treated as a fixed effect and *reaction time* as a random effect. The reaction time term was included to account for the inter-individual variability in the functional connectivity with respect to the subject performance (Hampson et al., 2010). In the model, the effect estimate (B_{ij}) for the *i*th subject ($i = 1, \ldots, 17$) in each condition (j = neutral, negative) is partitioned as

$$B_{ij} = \alpha 0_j + \alpha 1_j * \chi_{ij} + \Delta 0_i + \Delta_i * \chi_{ij} + \varepsilon_{ij}$$

where χ_{ij} is the RT of the *i*th subject in the *j*th condition, $\alpha 0_j$ is the group effect in the *j*th condition, $\alpha 1_j$ is the marginal group effect of RT under the *j*th condition, $\Delta 0_i$ and $\Delta_i \times \chi_{ij}$ represent the deviation of the linear fit of the *i*th subject, and ε_{ij} is the residual term. The effect of emotion in the linear mixed effect model was assessed separately for

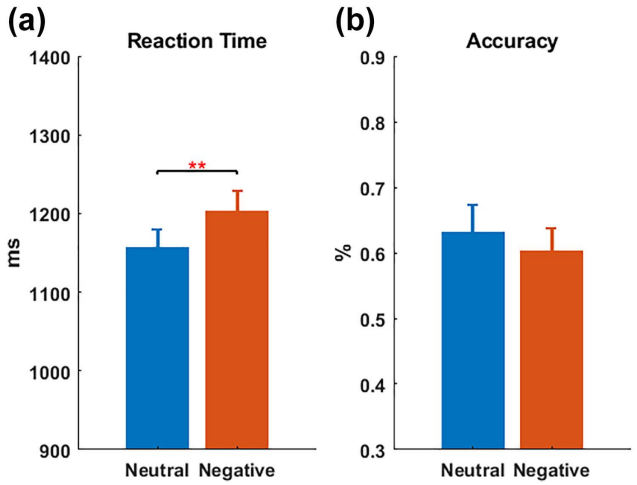

FIGURE 2 Behavioral results. Differences between the two conditions for (a) reaction time (**$p = .002$) and (b) accuracy ($p = .40$), using individualized conditions [Color figure can be viewed at wileyonlinelibrary.com]

each seed. Results have been corrected via Monte Carlo simulation as implemented in the AFNI program 3dClustSim, using a threshold of $p < .0075$ and a cluster size >20 voxels, to obtain a corrected significance level of $\alpha < 0.05$.

To test if interindividual variability in the emotional interference is related to functional connectivity modulations, we extracted β values obtained after gPPI from each seed-target pair that showed a modulation in the mixed effects models. For each pair, we tested the existence of a correlation between behavioral differences among conditions (ΔRT) and differences in functional connectivity. For each seed-target pair, the difference in connectivity was obtained by subtracting the beta value associated with the neutral condition from the beta value associated with the negative condition: $\Delta\beta_{fc} = \beta_{neg} - \beta_{neu}$.

Correlations with reaction times

In this analysis, we were specifically interested in the relation between behavioral performance and functional connectivity among task-activated and task-deactivated regions that was already described in previous studies for specific DMN regions (Hampson et al., 2010; Kelly et al., 2008). Correlation between connectivity and RT was assessed using Pearson correlation, separately for each seed, in the neutral condition. Results have been corrected via Monte Carlo simulation as implemented in the AFNI program 3dClustSim, using a threshold of $p < .025$ and a cluster size >20 voxels, to obtain a corrected significance level of $\alpha < 0.05$.

An ROI was created in the center of mass of each target for those clusters the connectivity of which was correlated with RT. Therefore, functional connectivity β values for each seed-target pair, in both neutral and negative conditions, were extracted and then correlated with RT. A bootstrap approach (Efron & Tibshirani, 1986) was used to estimate the difference between correlations in negative and neutral conditions: 1000 bootstrap samples were generated, and the Pearson correlation was computed between RT and functional connectivity for each sample and for each condition. To assess if emotional stimuli led to a different correlation between connectivity and RT, the effect size between the two z-transformed distributions of correlations was calculated using Cohen's *d* (J. Cohen, 1988). This procedure was repeated for each significant seed-target pair.

3 | RESULTS

3.1 | Behavioral results

The use of individual ratings led to the identification of 45 ± 4 (mean ± standard deviation) negative and 43 ± 4 neutral trials. The number of trials was not significantly different between conditions (paired samples *t* test, $p = .16$). After the individualization procedure, the mean score for valence across fMRI participants was 5.8 ± 1.2 for neutral images, and 2.0 ± 1.0 for negative images; the mean score for arousal was 3.9 ± 1.3 for neutral images, and 7.3 ± 1.2 for negative images the mean score for the *valence*arousal* dimensions was 2.6 ± 1.6 for neutral images, and −2.5 ± 1.4 for negative images. Consistency measured using Cronbach's Alpha revealed good internal consistencies in all cases (valence: $\alpha = 0.83$ for neutral and $\alpha = 0.77$ for negative condition; arousal: $\alpha = 0.84$ for neutral and $\alpha = 0.76$ for negative condition; *valence*arousal*: $\alpha = 0.87$ for neutral and $\alpha = 0.81$ for negative condition).

ANOVAs revealed a significant difference in RT between conditions, with negative trials showing a slower response ($p = .002$, $F = 10.9$, Figure 2). The difference in accuracy between negative and neutral trials was not significant ($p = .40$, $F = 0.7$). No significant effects were observed in the factor *trial type* ($p = .28$, $F = 1.2$ for RT; $p = .24$, $F = 1.4$ for accuracy), indicating no differences between *same* and *change* trials. The interaction between the two factors was not significant ($p = .54$, $F = 0.4$ for RT; $p = .60$, $F = 0.3$ for accuracy). Although differences in RT were also detectable using the nonindividualized trials, in the latter case the significance was smaller ($p = .02$, $F = 5.8$). Calculation of omega squared confirmed a larger effect in the case of individualized conditions (Table 1). Therefore, in the remaining analysis, we used individualized negative and neutral conditions.

The *emotion* × *block* ANOVA confirmed the effect of the emotional interference on RT ($p = .003$, $F = 9.6$). No effect was observed for the factor *block* ($p = .66$, $F = 0.5$), nor for the interaction ($p = .98$, $F = 0.1$), showing that the effect of the emotional interference was constant over the whole length of the task. The *emotion* × *block* ANOVA was not significant for the accuracy ($p = .73$, $F = 0.43$ for the

TABLE 1 Mean reaction times as estimated by individualized and standard trials

	RT ± SE (ms)	
	Individualized	**Standard**
Neutral	1158 ± 23	1148 ± 31
Negative	1203 ± 26	1187 ± 35
ω^2	0.161	0.086

Note. Effect sizes (ω^2) are indicated for the two methods. Notably, an effect size of 0.161 is considered a *large effect*, while 0.086 is considered a *medium effect*.

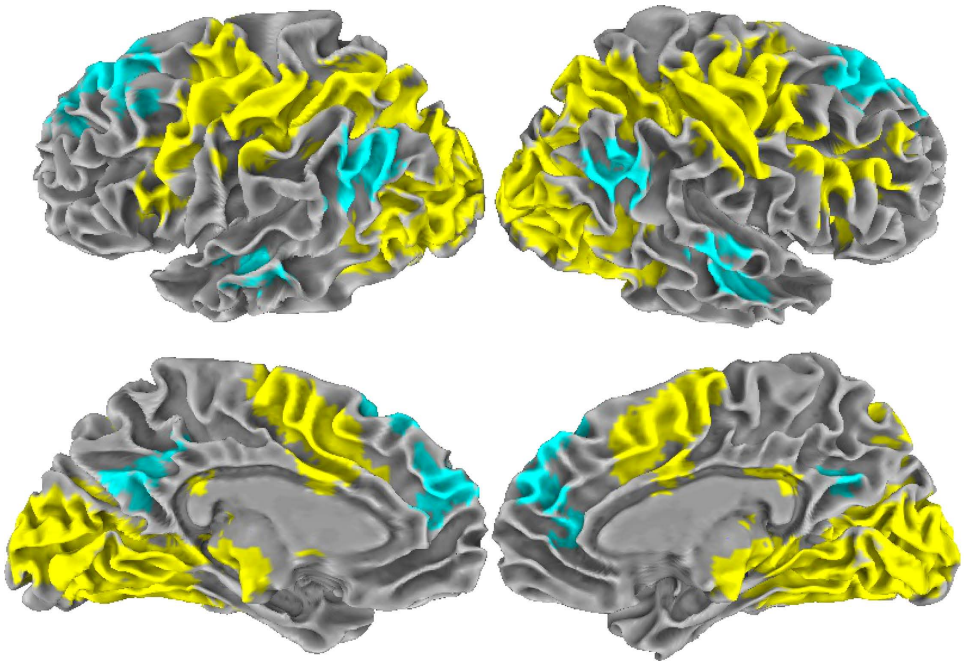

FIGURE 3 Task-related mask extracted using noise runs. Task-relevant activations are depicted in yellow, deactivations in cyan. Task-deactivated regions included posterior cingulate cortex (PCC), bilateral angular gyrus (AG), bilateral middle temporal gyrus (MTG), bilateral superior frontal gyrus (SFG), and medial prefrontal cortex (mPFC). Task-activated regions included: occipital lobe cortex, posterior temporal cortex, fusiform gyrus, intraparietal sulcus, superior parietal lobe, part of precentral and postcentral gyri, anterior mid-cingulate cortex, anterior insula, thalamus, midbrain structures, and part of inferior and middle frontal gyri in the right hemisphere [Color figure can be viewed at wileyonlinelibrary.com]

main effect of accuracy; $p = .24$, $F = 1.41$ for the main effect block; $p = .56$, $F = 0.7$ for the interaction).

3.2 | fMRI results

3.2.1 | Definition of a task-related mask

The analysis of noise trials identified 14,475 voxels showing task-related activation, and 1,954 voxels showing task-related deactivation ($\alpha \ll 0.01$, see Figure 3). Task-deactivated regions included regions of the DMN, that are usually deactivated in externally directed tasks (Shulman et al., 2003), such as posterior cingulate cortex (PCC), bilateral angular gyrus (AG), bilateral middle temporal gyrus (MTG), bilateral superior frontal gyrus (SFG), and medial prefrontal cortex (mPFC). Task-activated regions included regions usually associated with externally directed attention, visual stimuli detection, decision making, and motor response (M. D. Fox et al., 2005; Vanhaudenhuyse et al., 2011), such as occipital lobe cortex, posterior temporal cortex, fusiform gyrus, intraparietal sulcus, superior parietal lobe, part of precentral and postcentral gyri, anterior mid-cingulate cortex, anterior insula, thalamus, and midbrain structures. Notably, in the right hemisphere, also inferior and middle frontal gyri were activated. All the activations and deactivations here reported are included in the task-related mask used in the following analysis on neutral and negative trials.

3.2.2 | Activity in neutral and negative trials

During complete correct trials, activity was higher in negative complete trials than in the neutral ones in bilateral superior parietal lobule (l-SPL and r-SPL, $\alpha \ll 0.01$ for both). The activity in negative catch trials was higher in the right inferior frontal gyrus (r-IFG, pars opercularis, $\alpha < 0.01$), compared to neutral catch trials. Instead, in bilateral anterior lingual gyrus (l-aLG and r-aLG, $\alpha < 0.01$ for both), activity resulted to be higher in neutral catch trials, compared to negative catch trials (Figure 4a; see Table 2 for coordinates). All the regions the activity of which was modulated by emotions resulted therefore to be task-activated regions.

The timecourses of modulated RoI are visible in Figure 4b–f. Increased activity in parietal and frontal RoIs was confirmed in negative trials. T-tests revealed that in bilateral SPL this modulation was present in four timepoints, spanning from the first peak of activity to the second peak of activity (T3, T4, T5, T6), which are presumably associated with the sample and target presentation, respectively. In right IFG a higher activity in negative trials was observed only at the peak of activity associated with the sample presentation (T3). Increased activity in neutral trials was observed in bilateral aLG, where significant differences in two timepoints (T2 and T3) were found in both left and right aLG, although only results for left aLG remained significant after FDR correction. Modulations observed in right IFG and bilateral aLG during complete trials confirmed that the use of catch trials and complete trials allowed us to detect all the brain regions in which activity was modulated during one or more timepoints of the trial.

Timepoints of interest for correlation analysis were T3, T4, T5, and T6 for left and right SPL, T3 for right IFG, and T2 and T3 for left aLG. Results revealed inverse correlations between $\Delta\beta_{act}$ and ΔRT in the fifth timepoint (T5) for both parietal ROIs. After correction for multiple

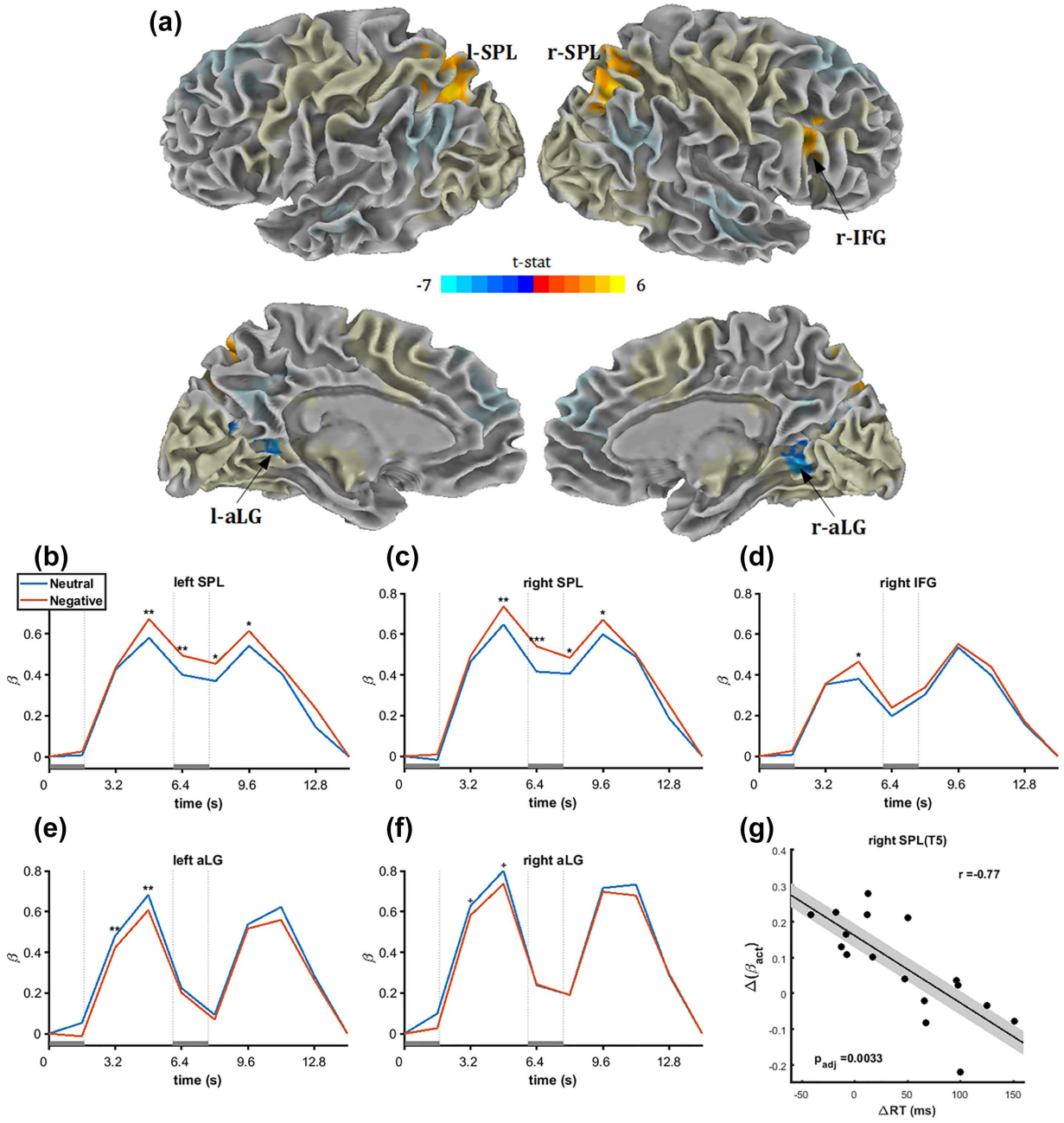

FIGURE 4 Timecourse analysis results. (a) Regions significantly modulated by emotion, superimposed on the task-related mask (shaded). Color intensity indicates *t*-statistic, as shown in the colorbar. (b–f) Timecourses extracted from the five clusters. Zero corresponds to sample onset; the two grey boxes indicate respectively the sample and the target presentations. Results for correct trials are shown. Timepoints significantly different between the two conditions are marked with asterisks (*$p < .05$, **$p < .01$, ***$p < .001$; +: n.s. after FDR correction). (g) Correlation between ΔRT and $\Delta\beta_{act}$ in right SPL, timepoint T5; regression line and standard errors (shaded) are shown. l/r-SPL = left/right superior parietal lobule; r-IFG = right inferior frontal gyrus; l/r-aLG = left/right anterior lingual gyrus [Color figure can be viewed at wileyonlinelibrary.com]

comparisons, however, only the result for right SPL maintained significance ($r = -.77$, $p_{adj} = .003$, bootstrapped confidence intervals: $-0.85 \sim -0.60$, Figure 4g).

3.2.3 | Functional connectivity: effect of emotion

The main effect of *emotion* revealed a significant modulation of functional connectivity between parietal and occipital task-activated seeds and temporal and frontal task-deactivated regions (Figure 5a,b; see Table 3 for coordinates). No effect of emotion was found for the connectivity of right IFG, meaning that the functional connectivity of this area with task-deactivated regions was not significantly different between neutral and negative trials.

The functional connectivity of both parietal seeds with left middle temporal gyrus (l-MTG) was significantly decreased in negative trials. Connectivity between right aLG seed and the dorsolateral part of right superior frontal gyrus (r-dlSFG) was increased in negative trials, as it was the connectivity between left aLG seed and left dlSFG. A control analysis, using task-activated regions as a mask, was conducted to

TABLE 2 Regions in which the activity is modulated by emotional interference

Cluster	X	Y	Z	A	Nvox
l-SPL (BA7)	20	69	41	≪0.01	174
r-SPL (BA7)	−23	69	42	≪0.01	208
r-IFG (BA6)	−44	−7	29	<0.01	103
l-aLG (BA18)	15	56	8	<0.01	135
r-aLG (BA18)	−17	56	7	< 0.01	64

Note. Abbreviations: BA = Brodmann Area; l/r-SPL = left/right superior parietal lobule; l/r-aLG = left/right anterior lingual gyrus; r-IFG = right inferior frontal gyrus.
Talairach's coordinates of the center of mass, corrected significance level, and number of voxels are reported for each modulated cluster.

assess if modulations in functional connectivity were exclusively between task-activated and task-deactivated areas. No significant modulation in connectivity due to emotions was observed in this case.

Correlation analysis revealed a relationship between the difference in connectivity ($\Delta\beta_{fc}$) and ΔRT, only for the seed-target pair right aLG–right dlSFG. The two parameters showed a direct correlation ($r = .56$, $p = .018$, bootstrapped confidence intervals: 0.20 ~ 0.84, Figure 5c).

3.2.4 | Functional connectivity: Correlations with reaction times

Pearson correlation between RT and functional connectivity in the neutral condition was significant only for right IFG (Figure 6a). Specifically, functional connectivity between right IFG and three task-deactivated regions, namely, left dlSFG, left angular gyrus (l-AG) and left posterior cingulate cortex (l-PCC), was directly correlated with RT ($\alpha < 0.01$, Figure 6b, see Table 4 for coordinates). Notably, the cluster in the left dlSFG found in this analysis is located medially and anteriorly compared to the one described in the previous paragraph, that is, the one which shows increased connectivity with occipital regions in negative trials. In the negative condition, these correlations between connectivity and RT were weaker: Cohen's *d* estimation after bootstrapping revealed a large effect for left dlSFG ($d = 0.72$) and a medium effect for left PCC ($d = 0.45$). Thus, in negative trials, the functional connectivity of these task-deactivated regions with right IFG exhibited a lower correlation with the behavioral performance than in the neutral condition. No effect was found for left AG ($d = 0.05$), indicating that its connectivity with right IFG showed a similar correlation with RT in both conditions. We repeated the analysis using different numbers of bootstrap samples (i.e., 100, 200, 500, 1,500, 2,000), obtaining equivalent results.

A control analysis was conducted using task-activated regions as a mask, to assess if correlations between functional connectivity and RT existed only between task-activated and task-deactivated regions. No significant correlations between connectivity and RT were observed in this case.

4 | DISCUSSION

During negative trials, in which subjects were significantly slower, activity was increased in bilateral SPL, a region known to be involved in the processing of spatial information (Burnod et al., 1999; Corbetta &

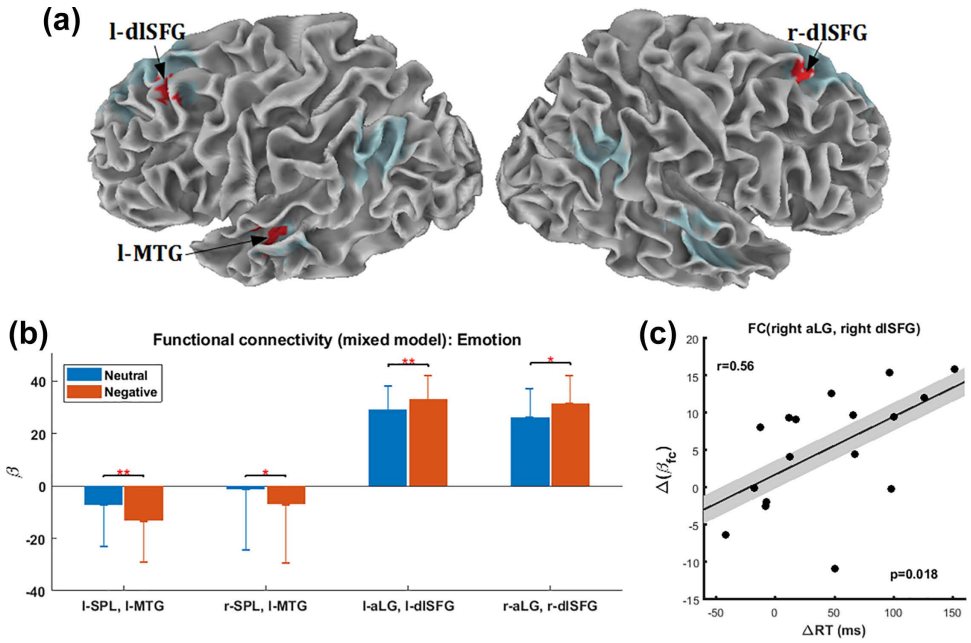

FIGURE 5 Functional connectivity: effect of emotion. (a) In red, task deactivated regions for which connectivity with parietal or occipital seeds is significantly modulated by emotion. (b) Mean connectivity β values obtained from gPPI, between the pairs of regions the connectivity of which was significantly modulated by emotion, in the mixed effects model. Differences in connectivity are marked with asterisks (*$\alpha < 0.05$, **$\alpha < 0.01$). (c) Correlation between ΔRT and $\Delta\beta_{fc}$ amidst right aLG and right dlSFG; regression line and standard errors (shaded) are shown. l/r-SPL = left/right superior parietal lobule; l/r-aLG = left/right anterior lingual gyrus; l-MTG = left middle temporal gyrus; l/r-dlSFG = left/right dorsolateral superior frontal gyrus [Color figure can be viewed at wileyonlinelibrary.com]

TABLE 3 Regions the connectivity of which is significantly modulated between conditions

Seed	Target	X	Y	Z	A
l-SPL	l-MTG (BA21)	51	19	−6	<0.01
r-SPL	l-MTG (BA21)	52	18	−5	<0.02
l-aLG	l-dlSFG (BA8)	27	−19	46	<0.01
r-aLG	r-dlSFG (BA8)	−25	−18	48	<0.03

Note. Abbreviations: l/r-SPL = left/right superior parietal lobule; l/r-aLG = left/right anterior lingual gyrus; l-MTG = left middle temporal gyrus; l/r-dlSFG = left/right dorsolateral superior frontal gyrus. Target coordinates and significance level for each pair of seed-target are shown.

Shulman, 2002), and in right IFG, a region of the cingulo-opercular network (Menon, 2011). In contrast, decreased activity during negative trials was found in bilateral aLG, a secondary visual area involved in visual attention and imagery (Kosslyn, Ganis, & Thompson, 2001; Leshikar, Duarte, & Hertzog, 2012). As we hypothesized, between negative and neutral conditions there was a different coupling among task-activated and task-deactivated areas, but not within task-activated regions. In particular, in negative trials, we observed (a) an increase in occipito-frontal functional connectivity between bilateral aLG and each corresponding ipsilateral dlSFG and (b) a decrease in parieto-temporal functional connectivity between bilateral SPL and left MTG.

Our results are in line with a recent study (Benedek et al., 2016) in which a similar topography of activation differences was found

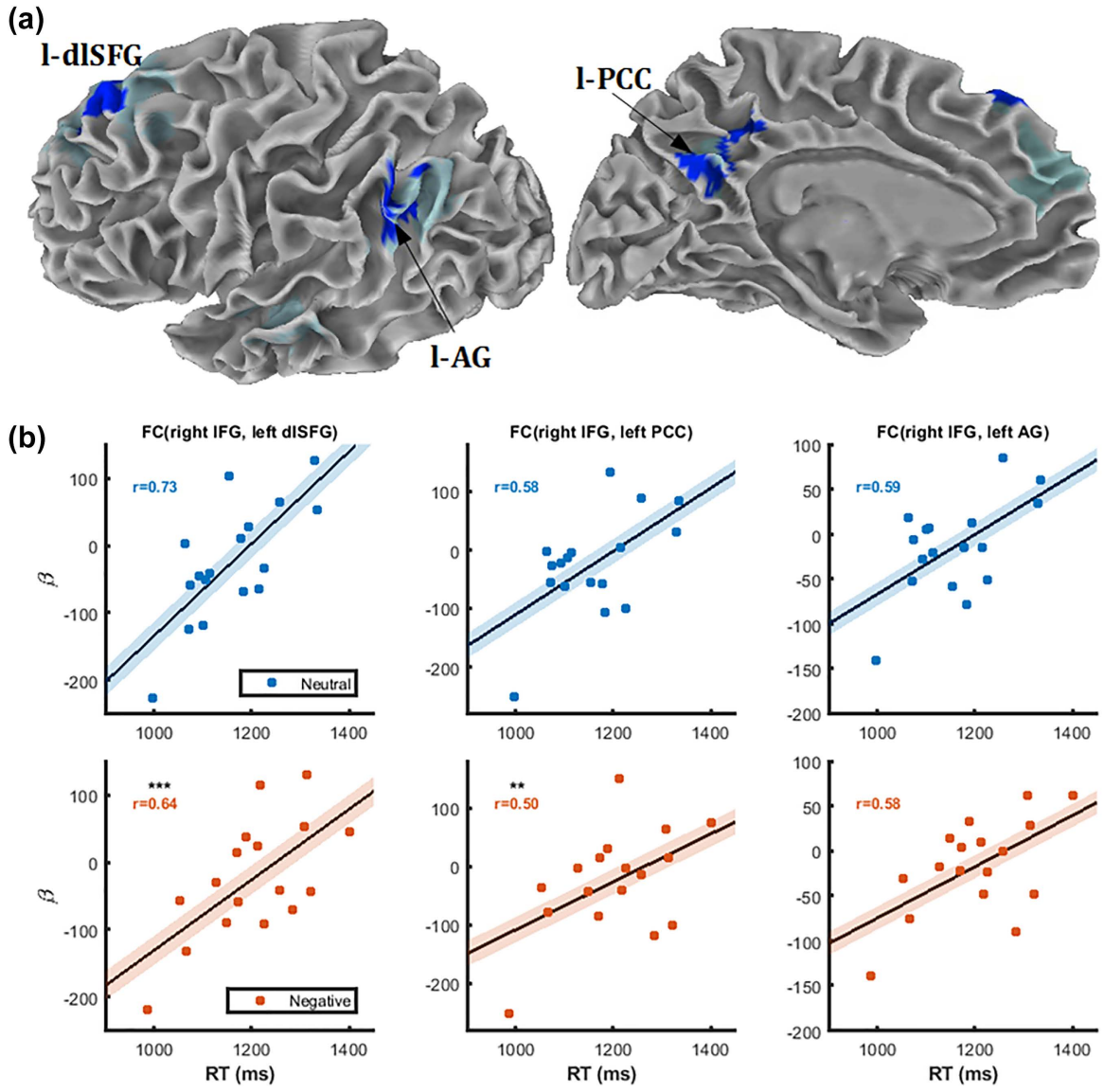

FIGURE 6 Functional connectivity: correlations with RT. (a) In blue, task-deactivated regions for which the connectivity with right IFG is significantly correlated with RT. (b) For each significant target, regression lines and correlation values are shown, for each condition. Differences in slopes, estimated using Cohen's *d* after bootstrap, are marked with asterisks (***$d > 0.5$, large effect; **$d > 0.3$ medium effect). r-IFG = right inferior frontal gyrus; l-dlSFG = left dorsolateral superior frontal gyrus; l-PCC = left posterior cingulate cortex; l-AG = left angular gyrus [Color figure can be viewed at wileyonlinelibrary.com]

TABLE 4 Regions for which the connectivity with right IFG is correlated to RT

Seed	Target	*X*	*Y*	*Z*	α
r-IFG	l-dlSFG (BA8)	16	−29	47	<0.01
r-IFG	l-AG (BA39)	46	58	30	<0.01
r-IFG	l-PCC (BA31)	6	53	29	<0.01

Note. Abbreviations: l-dlSFG = left dorsolateral superior frontal gyrus; l-AG = left angular gyrus; l-PCC = left posterior cingulate cortex; r-IFG = right inferior frontal gyrus.
Talairach's coordinates and corrected significance level are shown for each target.

contrasting an externally directed anagram task with an internally directed one. Interestingly, in our study the increase of activity in SPL was inversely correlated with the behavioral impairment associated with the emotional interference: the more SPL activity increased in negative trials with respect to neutral trials, the more the subject was likely to have a similar RT between the two conditions, thus not experiencing the interference effect. Importantly, the modulation of functional connectivity between right aLG and right dlSFG was related to the emotional interference in an opposite fashion with respect to the activity in SPL: the more the two regions showed higher coupling during negative trials than during neutral trials, the more the subject was likely to suffer the interference effect caused by negative stimuli. Our results demonstrate that the behavioral impairment caused by irrelevant emotional features of external stimuli during an externally oriented task relies both on the activity in regions related to the processing of spatial information and on the functional connections between visual areas and task-deactivated DMN frontal regions.

We found a link between functional connectivity and behavioral performance (RT) for connections between right IFG and several DMN regions in the left hemisphere (dlSFG, PCC, AG), but not for connections within task-activated regions. Interestingly, the strength of these correlations was heavily decreased in the negative condition for both left PCC and left dlSFG. The increase in activity observed in right IFG reflects the role of this area in the suppression of task-irrelevant regions (Chadick & Gazzaley, 2011; Menon, 2011). Indeed, it is conceivable that the observed anticorrelations between right IFG and DMN regions represent inhibitory modulations (Buckner et al., 2013; Gopinath, Krishnamurthy, Cabanban, & Crosson, 2015). In fact, as also other studies suggested (Hampson et al., 2010; Kelly et al., 2008), higher functional inhibition between control regions and the DMN indicates higher performance. The lower correlation between functional connectivity and RT found in negative trials is likely to indicate that inhibition toward the DMN is less effective during emotional stimulation. Considering anticorrelations between a positively engaged region (IFG) and several deactivated DMN regions (dlSFG, PCC, AG), it is likely that the activated region is driving the inhibition, and not vice versa. A recent study (Li et al., 2013) analyzed the anatomical and functional connectivity patterns of SFG subregions and found dlSFG to be anatomically connected with IFG and functionally coupled with both prefrontal areas and regions of the DMN, especially PCC. They conclude that dlSFG may serve as a connection node between medial limbic regions and executive networks. Our results support this hypothesis, suggesting that dlSFG may be a key region in favoring internally focused processes promoted by the DMN by attributing the appropriate amount of salience to the emotional features of visual inputs.

In contrast to the occipito-frontal coupling, we observed a decreased connectivity between bilateral SPL and left MTG in the negative condition. Previous studies have shown that the anterior temporal cortex is related to social cognition and theory of mind (Buckner et al., 2008; Soch et al., 2016) and that its connectivity may be altered in pathologies associated with social impairments (Abram et al., 2017; Zilbovicius et al., 2006). Presumably, in negative trials, the rise of the emotional load increases the likelihood of social information to be processed by the temporal cortex. In this framework, the increased anticorrelation between temporal and parietal regions may reflect an increased inhibition toward the processing of irrelevant social information.

Our findings show that functional connections between task-activated and task-deactivated (DMN) brain regions mediate the effects of the emotional interference. Among the involved DMN regions, PCC and especially dlSFG are likely to play a crucial role in the attribution of salience to internally focused processes due to their connections with both DMN and executive regions. On the other hand, SPL and IFG are crucial in maintaining externally oriented attention, confirming results from a previous meta-analysis on working memory subprocesses (Nee et al., 2013). Mechanisms mediated by the emotional interference through DMN connections probably derive from the evolutionary advantages in following orientations provided by internal feelings when inputs with high arousal are perceived (Damasio & Carvalho, 2013). Indeed, albeit ignoring irrelevant information is useful to increase efficiency, if a task-irrelevant stimulus has high emotional content—suggesting a dangerous situation—the interference mediated by the DMN favors the switch from the task execution to a behavioral response aimed at neutralizing the threat or safeguarding the self. The existence of such evolutionary useful mechanism, mediated by task-deactivated brain regions during externally-directed behavior, contributes to blur the definition of a "task-negative" network.

Many studies demonstrated that the use of the "task-negative" versus "task-positive" dichotomy might be misleading (Andrews-Hanna et al., 2014; Anticevic et al., 2012; Callard & Margulies, 2014; Spreng, Stevens, Chamberlain, Gilmore, & Schacter, 2010). Here, we extend this evidence showing that (a) task-deactivated regions, although not directly modulated in their activity, exhibit a different degree of coupling with task-activated areas between conditions and (b) the emotional interference is predicted not only by the activity in task-activated regions but also by the coupling between task-activated and task-deactivated regions.

Importantly, in our study, we found a pattern of deactivated brain regions the connectivity of which is correlated with the emotional interference and with the behavioral performance. Most of these task-deactivated regions were in the left hemisphere. To note, we used a spatial attention task, which involves active processes mainly distributed over the right hemisphere (Champod & Petrides, 2007; Corbetta & Shulman, 2011). Crucial top–down modulations have been found to

be predominantly interhemispheric (Knyazeva et al., 1999; Szczepanski, Pinsk, Douglas, Kastner, & Saalmann, 2013), but intrahemispheric as well (Szczepanski, Konen, & Kastner, 2010; Thiebaut de Schotten et al., 2011). We suggest that topographies of activations and deactivations showing such modulations represent task-specific phenomena, and the degree of internally versus externally directed information demanded by the task is likely to play a critical role in this interplay.

4.1 | Limitations

Our study is not without limitations though. First, in our emotional interference paradigm, we included neutral and negative stimuli, but not positive ones. Thus, our results related to the emotional interference are referred to the effects exerted by negative emotions. However, focusing only on two conditions allowed us to include a high number of trials for each condition, which was a benefit to the study. Second, as in most emotion-related paradigms, emotional stimuli used in our study can evoke verbal thoughts, which may interfere with the aim of the experiment. To minimize this effect, task difficulty was individualized through the preliminary section, and individuals with poor performances were excluded, ensuring a substantial engagement subjects' spatial attention, disfavoring other cognitive modalities. Third, extracting a *valence*arousal* principal component to analyze data implies that we cannot distinguish between effects exerted by valence or arousal, separately. However, we demonstrated that the individualization procedure performed using PCA successfully caught the effect of the emotional interference better than using the standard neutral vs negative classification. Conceivably, future studies will support the usefulness of the PCA, or discuss its incorrectness, when dealing with a dimensional approach to the study of emotions.

4.2 | Conclusions

Our results show that the resistance against the emotional interference relies on the activity in task-activated regions as well as on the connectivity between these regions and task-deactivated DMN areas related to social cognition and internally focused processes. This suggests that the shift from externally directed attention toward internal mentation is related to the interplay between these two sets of regions. Moreover, we have shown that anticorrelations may be an indicator of inhibition patterns and may impact the behavioral performance depending on the emotional content of visual stimuli.

Further studies are needed to further investigate these mechanisms in different contexts. For example, it would be interesting to evaluate the interference of nonrelevant external stimuli during internally focused processes (i.e., autobiographical tasks, meditative states). Additionally, orthogonal linguistic tasks may help understanding if topographies of functional inhibitions related to behavioral performance are task-specific and predominantly inter-hemispheric. Finally, functional connections of the DMN are altered in several psychiatric disorders associated with a disrupted interplay between internal mentation and externally directed attention. We have shown here that specific DMN regions (i.e., dlSFG, PCC) may play an essential role in the attribution of salience to internally directed processes. Thus, the investigation of such interplay should be conducted not only using predefined networks but investigating the contribution of single regions abnormalities to each disorder.

CONFLICT OF INTEREST

The authors declare no competing financial interests.

ORCID

Simone Di Plinio http://orcid.org/0000-0002-2551-0985

REFERENCES

Abram, S. V., Wisner, K. M., Fox, J. M., Barch, D. M., Wang, L., Csernansky, J. G., … Smith, M. J. (2017). Fronto-temporal connectivity predicts cognitive empathy deficits and experiential negative symptoms in schizophrenia. *Human Brain Mapping*, *38*(3), 1111–1124. https://doi.org/10.1002/hbm.23439

Andrews-Hanna, J. R., Smallwood, J., & Spreng, R. N. (2014). The default network and self-generated thought: Component processes, dynamic control, and clinical relevance. *Annals of the New York Academy of Sciences*, *1316*(1), 29–52. https://doi.org/10.1111/nyas.12360

Anticevic, A., Cole, M. W., Murray, J. D., Corlett, P. R., Wang, X. J., & Krystal, J. H. (2012). The role of default network deactivation in cognition and disease. *Trends in Cognitive Sciences*, *16*(12), 584–592. https://doi.org/10.1016/j.tics.2012.10.008

Bado, P., Engel, A., de Oliveira-Souza, R., Bramati, I. E., Paiva, F. F., Basilio, R., … Moll, J. (2014). Functional dissociation of ventral frontal and dorsomedial default mode network components during resting state and emotional autobiographical recall. *Human Brain Mapping*, *35*(7), 3302–3313. https://doi.org/10.1002/hbm.22403

Benedek, M., Jauk, E., Beaty, R. E., Fink, A., Koschutnig, K., & Neubauer, A. C. (2016). Brain mechanisms associated with internally directed attention and self-generated thought. *Scientific Reports*, *6*(1), 22959. https://doi.org/10.1038/srep22959

Benjamini, Y., & Hochberg, Y. (1995). Controlling the false discovery rate: A practical and powerful approach to multiple testing. *Journal of the Royal Statistical Society*, *57*(1), 289–300. https://doi.org/10.2307/2346101

Biele, C., & Grabowska, A. (2006). Sex differences in perception of emotion intensity in dynamic and static facial expressions. *Experimental Brain Research*, *171*(1), 1–6. https://doi.org/10.1007/s00221-005-0254-0

Buckner, R. L., Andrews-Hanna, J. R., & Schacter, D. L. (2008). The brain's default network: Anatomy, function, and relevance to disease. *Annals of the New York Academy of Sciences*, *1124*(1), 1–38. https://doi.org/10.1196/annals.1440.011

Buckner, R. L., Krienen, F. M., & Yeo, B. T. (2013). Opportunities and limitations of intrinsic functional connectivity MRI. *Nature Neuroscience*, *16*(7), 832–837. https://doi.org/10.1038/nn.3423

Buodo, G., Sarlo, M., & Palomba, D. (2002). Attentional resources measured by reaction times highlight differences within pleasant and unpleasant, high arousing stimuli. *Motivation and Emotion*, *26*(2), 123–138.

Burnod, Y., Baraduc, P., Battaglia-Mayer, A., Guigon, E., Koechlin, E., Ferraina, S., … Caminiti, R. (1999). Parieto-frontal coding of reaching: An integrated framework. *Experimental Brain Research*, *129*(3), 0325–0346.

Callard, F., & Margulies, D. S. (2014). What we talk about when we talk about the default mode network. *Frontiers in Human Neuroscience*, *8*, 619. https://doi.org/10.3389/fnhum.2014.00619

Carretié, L., Hinojosa, J. A., & Mercado, F. (2003). Cerebral patterns of attentional habituation to emotional visual stimuli. *Psychophysiology*, *40*(3), 381–388.

Catani, M., Dell'acqua, F., & Thiebaut de Schotten, M. (2013). A revised limbic system model for memory, emotion and behaviour. *Neuroscience & Biobehavioral Reviews*, *37*(8), 1724–1737. https://doi.org/10.1016/j.neubiorev.2013.07.001

Chadick, J. Z., & Gazzaley, A. (2011). Differential coupling of visual cortex with default or frontal-parietal network based on goals. *Nature Neuroscience*, *14*(7), 830–832. https://doi.org/10.1038/nn.2823

Champod, A. S., & Petrides, M. (2007). Dissociable roles of the posterior parietal and the prefrontal cortex in manipulation and monitoring processes. *Proceedings of the National Academy of Sciences of the United States of America*, *104*(37), 14837–14842.

Chen, G., Saad, Z. S., Adleman, N. E., Leibenluft, E., & Cox, R. W. (2015). Detecting the subtle shape differences in hemodynamic responses at the group level. *Frontiers in Neuroscience*, *9*, 375. https://doi.org/10.3389/fnins.2015.00375

Chen, G., Saad, Z. S., Britton, J. C., Pine, D. S., & Cox, R. W. (2013). Linear mixed-effects modeling approach to FMRI group analysis. *NeuroImage*, *73*, 176–190. https://doi.org/10.1016/j.neuroimage.2013.01.047

Cohen, J. (1988). *Statistical power analysis for the behavioral sciences* (2nd ed.). Lawrence Erlbaum Associates.

Cohen, N., & Henik, A. (2012). Do irrelevant emotional stimuli impair or improve executive control?. *Frontiers in Integrative Neuroscience*, *6*, 33. https://doi.org/10.3389/fnint.2012.00033

Corbetta, M., & Shulman, G. L. (2002). Control of goal-directed and stimulus-driven attention in the brain. *Nature Reviews. Neuroscience*, *3*(3), 201–215. https://doi.org/10.1038/nrn755

Corbetta, M., & Shulman, G. L. (2011). Spatial neglect and attention networks. *Annual Review of Neuroscience*, *34*(1), 569–599. https://doi.org/10.1146/annurev-neuro-061010-113731

Cox, R. W. (1996). AFNI: Software for analysis and visualization of functional magnetic resonance neuroimages. *Computers and Biomedical Research*, *29*(3), 162–173.

Cox, R. W., Chen, G., Glen, D. R., Reynolds, R. C., & Taylor, P. A. (2017). FMRI clustering in AFNI: False positive rates redux. *Brain Connectivity*, *7*(3), 152–134.

Damasio, A., & Carvalho, G. B. (2013). The nature of feelings: Evolutionary and neurobiological origins. *Nature Reviews. Neuroscience*, *14*(2), 143–152. https://doi.org/10.1038/nrn3403

Dolcos, F., Wang, L., & Mather, M. (2014). Current research and emerging directions in emotion-cognition interactions. *Frontiers in Integrative Neuroscience*, *8*, 83. https://doi.org/10.3389/fnint.2014.00083

Efron, B., & Tibshirani, R. (1986). Bootstrap methods for standard errors, confidence intervals, and other measures of statistical accuracy. *Statistical Science*, *1*(1), 54–75.

Elton, A., & Gao, W. (2015). Task-positive functional connectivity of the default mode network transcends task domain. *Journal of Cognitive Neuroscience*, *27*(12), 2369–2381. https://doi.org/10.1162/jocn_a_00859

Filkowski, M. M., Olsen, R. M., Duda, B., Wanger, T. J., & Sabatinelli, D. (2017). Sex differences in emotional perception: Meta-analysis of divergent activation. *NeuroImage*, *147*, 925–933. https://doi.org/10.1016/j.neuroimage.2016.12.016

Fox, K. C., Spreng, R. N., Ellamil, M., Andrews-Hanna, J. R., & Christoff, K. (2015). The wandering brain: Meta-analysis of functional neuroimaging studies of mind-wandering and related spontaneous thought processes. *NeuroImage*, *111*, 611–621. https://doi.org/10.1016/j.neuroimage.2015.02.039

Fox, M. D., Snyder, A. Z., Vincent, J. L., Corbetta, M., Van Essen, D. C., & Raichle, M. E. (2005). The human brain is intrinsically organized into dynamic, anticorrelated functional networks. *Proceedings of the National Academy of Sciences of the United States of America*, *102*(27), 9673–9678. https://doi.org/10.1073/pnas.0504136102

Gopinath, K., Krishnamurthy, V., Cabanban, R., & Crosson, B. A. (2015). Hubs of anticorrelation in high-resolution resting-state functional connectivity network architecture. *Brain Connectivity*, *5*(5), 267–275. https://doi.org/10.1089/brain.2014.0323

Gorban, A. N., Kégl, B., Wunsch, D. C., & Zinovyev, A. (2008). *Principal manifolds for data visualization and dimension reduction*. Springer Ed.

Greicius, M. D., Krasnow, B., Reiss, A. L., & Menon, V. (2003). Functional connectivity in the resting brain a network analysis of the default mode hypothesis. *Proceedings of the National Academy of Sciences of the United States of America*, *100*(1), 253–258.

Grossmann, I., Ellsworth, P. C., & Hong, Y. Y. (2012). Culture, attention, and emotion. *Journal of Experimental Psychology: General*, *141*(1), 31–36. https://doi.org/10.1037/a0023817

Gusnard, D. A., & Raichle, M. E. (2001). Searching for a baseline functional imaging and the resting human brain. *Nature Reviews. Neuroscience*, *2*(10), 685–694.

Gutentag, T., Halperin, E., Porat, R., Bigman, Y. E., & Tamir, M. (2016). Successful emotion regulation requires both conviction and skill: Beliefs about the controllability of emotions, reappraisal, and regulation success. *Cognition & Emotion*, 1–9. https://doi.org/10.1080/02699931.2016.1213704

Hamann, S. (2012). Mapping discrete and dimensional emotions onto the brain: Controversies and consensus. *Trends in Cognitive Sciences*, *16*(9), 458–466. https://doi.org/10.1016/j.tics.2012.07.006

Hampson, M., Driesen, N., Roth, J. K., Gore, J. C., & Constable, R. T. (2010). Functional connectivity between task-positive and task-negative brain areas and its relation to working memory performance. *Magnetic Resonance Imaging*, *28*(8), 1051–1057. https://doi.org/10.1016/j.mri.2010.03.021

Kelly, A. M., Uddin, L. Q., Biswal, B. B., Castellanos, F. X., & Milham, M. P. (2008). Competition between functional brain networks mediates behavioral variability. *NeuroImage*, *39*(1), 527–537. https://doi.org/10.1016/j.neuroimage.2007.08.008

Knyazeva, M. G., Kiper, D. C., Vildavski, P. A., Despland, P. A., Maeder-Ingvar, M., & Innocenti, G. M. (1999). Visual stimulus – Dependent changes in interhemispheric EEG coherence in humans. *Journal of Neurophysiology*, *82*(6), 3095–3107.),

Kosslyn, S. M., Ganis, G., & Thompson, W. L. (2001). Neural foundations of imagery. *Nature Reviews. Neuroscience*, *2*(9), 635–642.

Leech, R., Scott, G., Carhart-Harris, R., Turkheimer, F., Taylor-Robinson, S. D., & Sharp, D. J. (2014). Spatial dependencies between large-scale brain networks. *PLoS One*, *9*(6), e98500.

Leshikar, E. D., Duarte, A., & Hertzog, C. (2012). Task-selective memory effects for successfully implemented encoding strategies. *PLoS One*, *7*(5), e38160. https://doi.org/10.1371/journal.pone.0038160

Li, B., Wang, X., Yao, S., Hu, D., & Friston, K. (2012). Task-dependent modulation of effective connectivity within the default mode network. *Frontiers in Psychology*, *3*, 206. https://doi.org/10.3389/fpsyg.2012.00206

Li, W., Qin, W., Liu, H., Fan, L., Wang, J., Jiang, T., & Yu, C. (2013). Subregions of the human superior frontal gyrus and their connections. *NeuroImage*, *78*, 46–58. https://doi.org/10.1016/j.neuroimage.2013.04.011

Lindquist, K. A., & Barrett, L. F. (2012). A functional architecture of the human brain: Emerging insights from the science of emotion. *Trends in Cognitive Sciences*, *16*(11), 533–540. https://doi.org/10.1016/j.tics.2012.09.005

Marchewka, A., Żurawski, Ł., Jednoróg, K., & Grabowska, A. (2014). The Nencki Affective Picture System (NAPS): Introduction to a novel, standardized, wide-range, high-quality, realistic picture database. *Behavior Research Methods*, *46*(2), 596–610. https://doi.org/10.3758/s13428-013-0379-1)

McLaren, D. G., Ries, M. L., Xu, G., & Johnson, S. C. (2012). A generalized form of context-dependent psychophysiological interactions (gPPI): A comparison to standard approaches. *NeuroImage*, *61*(4), 1277–1286. https://doi.org/10.1016/j.neuroimage.2012.03.068

McRae, K., Hughes, B., Chopra, S., Gabrieli, J. D., Gross, J. J., & Ochsner, K. N. (2010). The neural bases of distraction and reappraisal. *Journal of Cognitive Neuroscience*, *22*(2), 248–262. https://doi.org/10.1162/jocn.2009.21243

Menon, V. (2011). Large-scale brain networks and psychopathology: A unifying triple network model. *Trends in Cognitive Sciences*, *15*(10), 483–506. https://doi.org/10.1016/j.tics.2011.08.003

Most, S. B., Chun, M. M., Johnson, M. R., & Kiehl, K. A. (2006). Attentional modulation of the amygdala varies with personality. *NeuroImage*, *31*(2), 934–944. https://doi.org/10.1016/j.neuroimage.2005.12.031

Nee, D. E., Brown, J. W., Askren, M. K., Berman, M. G., Demiralp, E., Krawitz, A., & Jonides, J. (2013). A meta-analysis of executive components of working memory. *Cerebral Cortex*, *23*(2), 264–282. https://doi.org/10.1093/cercor/bhs007

Northoff, G., Heinzel, A., Bermpohl, F., Niese, R., Pfennig, A., Pascual-Leone, A., & Schlaug, G. (2004). Reciprocal modulation and attenuation in the prefrontal cortex: An fMRI study on emotional-cognitive interaction. *Human Brain Mapping*, *21*(3), 202–212. https://doi.org/10.1002/hbm.20002

Ochsner, K. N., Silvers, J. A., & Buhle, J. T. (2012). Functional imaging studies of emotion regulation: A synthetic review and evolving model of the cognitive control of emotion. *Annals of the New York Academy of Sciences*, *1251*(1), E1–24. https://doi.org/10.1111/j.1749-6632.2012.06751.x

Olejnik, S., & Algina, J. (2003). Generalized eta and omega squared statistics: Measures of effect size for some common research designs. *Psychological Methods*, *8*(4), 434–447. https://doi.org/10.1037/1082-989X.8.4.434

Raichle, M. E. (1998). Behind the scenes of functional brain imaging: A historical and physiological perspective. *Proceedings of the National Academy of Sciences of the United States of America*, *95*(3), 765–772.

Russell, J. A. (2009). Emotion, core affect, and psychological construction. *Cognition & Emotion*, *23*(7), 1259–1283. https://doi.org/10.1080/02699930902809375

Schneider, W., Eschman, A., & Zuccolotto, A. (2012). E-Prime 2.0 Reference Guide Manual.

Schimmack, U. (2005). Attentional interference effects of emotional pictures: Threat, negativity, or arousal? *Emotion*, *5*(1), 55–66. https://doi.org/10.1037/1528-3542.5.1.55

Shulman, G. L., Fiez, J. A., Corbetta, M., Buckner, R. L., Miezin, F. M., Raichle, M. E., & Petersen, S. E. (1997). Common blood flow changes across visual tasks: II. Decreases in cerebral cortex. *Journal of Cognitive Neuroscience*, *9*(5), 648–663. https://doi.org/10.1162/jocn.1997.9.5.648.

Shulman, G. L., McAvoy, M. P., Cowan, M. C., Astafiev, S. V., Tansy, A. P., D'Avossa, G., & Corbetta, M. (2003). Quantitative analysis of attention and detection signals during visual search. *Journal of Neurophysiology*, *90*(5), 3384–3397.

Singh, K. D., & Fawcett, I. P. (2008). Transient and linearly graded deactivation of the human default-mode network by a visual detection task. *NeuroImage*, *41*(1), 100–112. https://doi.org/10.1016/j.neuroimage.2008.01.051

Soch, J., Deserno, L., Assmann, A., Barman, A., Walter, H., Richardson-Klavehn, A., & Schott, B. H. (2016). Inhibition of information flow to the default mode network during self-reference versus reference to others. *Cerebral Cortex*, https://doi.org/10.1093/cercor/bhw206.

Spreng, R. N. (2012). The fallacy of a "task-negative" network. *Frontiers in Psychology*, *3*, 145. https://doi.org/10.3389/fpsyg.2012.00145

Spreng, R. N., Stevens, W. D., Chamberlain, J. P., Gilmore, A. W., & Schacter, D. L. (2010). Default network activity, coupled with the frontoparietal control network, supports goal-directed cognition. *NeuroImage*, *53*(1), 303–317. https://doi.org/10.1016/j.neuroimage.2010.06.016

Supek, S., & Aine, C. J. (2014). *Magnetoencephalography: From signals to dynamic cortical networks*. Springer.

Szczepanski, S. M., Konen, C. S., & Kastner, S. (2010). Mechanisms of spatial attention control in frontal and parietal cortex. *Journal of Neuroscience*, *30*(1), 148–160. https://doi.org/10.1523/JNEUROSCI.3862-09.2010

Szczepanski, S. M., Pinsk, M. A., Douglas, M. M., Kastner, S., & Saalmann, Y. B. (2013). Functional and structural architecture of the human dorsal frontoparietal attention network. *Proceedings of the National Academy of Sciences of the United States of America*, *110*(39), 15806–15811.

Talairach, J., & Tournoux, P. (1988). *Co-planar stereotaxic atlas of the human brain*. Thieme Medical Publishers.

Thiebaut de Schotten, M., Dell'Acqua, F., Forkel, S. J., Simmons, A., Vergani, F., Murphy, D. G., & Catani, M. (2011). A lateralized brain network for visuospatial attention. *Nature Neuroscience*, *14*(10), 1245–1246. https://doi.org/10.1038/nn.2905

Troncoso Skidmore, S., & Thompson, B. (2013). Bias and precision of some classical ANOVA effect sizes when assumptions are violated. *Behavior Research Methods*, *45*(2), 536–546. https://doi.org/10.3758/s13428-012-0257-2

Vanhaudenhuyse, A., Demertzi, A., Schabus, M., Noirhomme, Q., Bredart, S., Boly, M., ... Laureys, S. (2011). Two distinct neuronal networks mediate the awareness of environment and of self. *Journal of Cognitive Neuroscience*, *23*(3), 570–578.

Zilbovicius, M., Meresse, I., Chabane, N., Brunelle, F., Samson, Y., & Boddaert, N. (2006). Autism, the superior temporal sulcus and social perception. *Trends in Neurosciences*, *29*(7), 359–366. https://doi.org/10.1016/j.tins.2006.06.004

How to cite this article: Di Plinio S, Ferri F, Marzetti L, Romani GL, Northoff G, Pizzella V. Functional connections between activated and deactivated brain regions mediate emotional interference during externally directed cognition. *Hum Brain Mapp*. 2018;39:3597–3610. https://doi.org/10.1002/hbm.24197